

# Model-based form error compensation in the turning of thin-walled cylindrical parts

U. Heisel · C. Kang

Received: 28 July 2010 / Accepted: 24 November 2010 / Published online: 14 December 2010  
© German Academic Society for Production Engineering (WGP) 2010

**Abstract** The turning of thin-walled, hollow, cylindrical parts is often not possible when using the common hydraulically operated 3- or 4-jaw chucks. This is due to the deformation of the part by the clamping force of the chuck. Even low clamping forces cause elastic deformations of the clamped workpiece, which results in surface errors due to machining after the unclamping and elastic recovery of the part. For this reason, several approaches have been adopted in the past in order to quantify and minimise the clamping-induced deformations. In this paper a model-based error compensation for thin-walled, cylindrical parts in turning is presented as a universal solution. In this work, a compensation by different models is designed and realised by an intelligent, adaptive and interchangeable turning tool holder with integrated sensors and actuators.

**Keywords** Thin-walled · Cylindrical · Model-based compensation · Adaptive

## 1 Introduction

### 1.1 Outset

In the clamping of thin-walled, elastic parts in the jaw chuck of a lathe, undesirable but generally elastic deformations of the workpiece occur, which cause a deviation of the clamped outer surface of the workpiece from the ideal round outer surface. The deformation of the workpiece due

to clamping forces is dependent on the workpiece and clamping geometry, Fig. 1 left. If such a deformed workpiece is machined with a stiff lathe, the desired round surface is indeed generated on the clamped workpiece, but after unclamping, a permanent form deviation of the machined surface occurs due to the elastic recovery. Another effect in the machining of very elastic workpieces is the deformation of the workpiece by the acting resultant forces, Fig. 1 right. It is dependent on the workpiece geometry and on the current position of the tool. Due to the position-dependent elasticity of the workpiece, this causes surface errors as a result of the varying cutting depth. The elasticity of the workpiece at the projecting end is higher than close to the clamping, which causes surface errors.

Thus, two deformation states exist that interfere with each other: the clamping force-induced deformation of the workpiece, which revolves with the workpiece, and the resultant force-induced deformation, which remains quasi-stationary from the point of view of the tool. Both states are in complex dynamic interaction during the cutting process, which causes variable stability conditions up to instability.

Currently, there are solutions, such as e.g. clamping systems with a specifically constructive design. Examples are systems with elastomer components [1] or six-point pendulum chuck clamping devices [2], in which the parts can be clamped with only little deformation. So-called membrane clampings also allow a uniform clamping of workpieces without deformation [3]. A distortion-free clamping of thin parts can also be achieved with vacuum clamping systems. Universal round chucks for the machining of unstable and thin discs are available especially for lathes [4]. Further designs are based on locking plates, plates with holes, vacuum plates attached to the workpiece-independent, plates with intake opening, vacuum-combs and plates with sintered metal overlay [5].

---

U. Heisel (✉) · C. Kang  
Institute for Machine Tools, University of Stuttgart,  
Holzgartenstraße 17, 70174 Stuttgart, Germany  
e-mail: heisel@ifw.uni-stuttgart.de

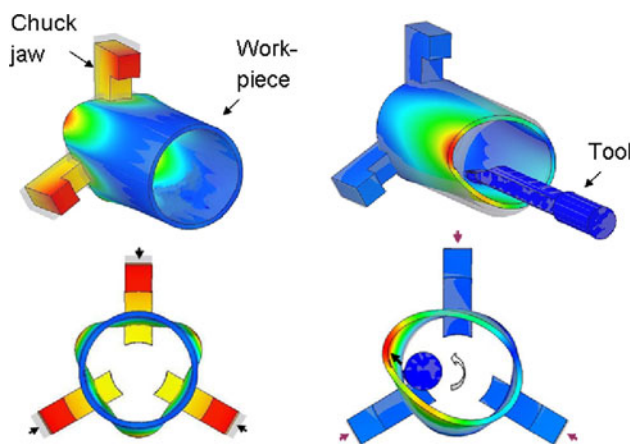


**Fig. 1** FEM-Simulation of the deformation of the thin-walled workpiece under clamping pressure (*left*) and with additional action of the resultant force vector (*right*)

These solutions, however, are very specific systems, which are not universally applicable and at the same time cause a great setup effort.

In the clamping of thin-walled hollow cylinders the narrow range between the minimum clamping force to take up the static and dynamic machining forces and the maximum clamping force with significant deformation of the part can be calculated [6] and used as input values for an adaptive clamping system [7]. The elastic form variations could be demonstrated in [8] by means of FE-simulation for different clamping systems and cutting conditions [9]. Work on the modelling of deformations is described in [10].

## 1.2 Objectives

In the present work a model-based compensation for form errors is to be developed. These errors occur on thin-walled and hence very elastic turning workpieces by clamping and deforming the workpiece under the currently acting resultant forces.

To eliminate undesirable vibration phenomena and dynamic instabilities in the turning process from the outset, the surface errors on the workpiece should also be measured—possibly even during machining—and the resulting cutting force variations should be determined. Particularly self-excited chatter phenomena in inner-cylindrical turning, in which extremely slim and elastic tools are used in addition to the thin-walled elastic workpiece, represent a recurring problem in practice. To solve the problem, a dynamic investigation is required, which takes into account the characteristics of the machine, the elastic workpiece and the elastic tool. The high feed dynamics, which is necessary for the compensation, cannot be provided by the machine axis. Hence, the future vision is an adaptive,

intelligent and interchangeable turning tool with integrated sensors and actuators.

The aim is a lathe capable of reacting flexibly and adaptively to given surface errors and extremely elastic workpieces. This research project lays the foundation for implementing this vision in everyday production engineering. The long-term goal is to transfer the gained solutions to a machine tool for the manufacturing of thin-walled turning parts.

## 2 Research project

### 2.1 Selection and adaptation of a suitable measuring principle

The measurement within the working environment contaminated by cutting fluid and chips puts special demands on the robustness and insensitivity of the measurement system. There are basically two options to measure the workpiece geometry: the contact measurement by means of measuring sensors or similar and the non-contact scanning of the surface, for example with laser sensors or inductive and capacitive measuring sensors. Within the project the surface should be measured without contact so as not to affect the workpiece. In comparative tests, generally potential measurement systems should be investigated and evaluated. Possible non-contact measuring methods are eddy current sensors, capacitive distance sensors and laser triangulation systems (Fig. 2).

Optical laser systems provide a high-precision and a high-resolution, but are susceptible to dirt, beam disturbances caused by dust and particles and overflow with cutting fluid. Capacitive sensors provide high resolutions, but are very sensitive to environmental influences, impurities, dielectrics and dirt at the measuring point.

Eddy current sensors are wear and maintenance free. Dirt, dust, humidity, oil and dielectric materials in the measuring gap do not cause any measuring errors. Metallic particles and adhesions can, for example, be blocked by an

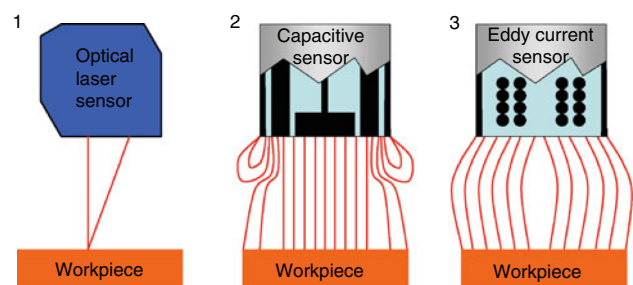


**Fig. 2** Optical laser sensor (*left*), capacitive sensor (*middle*) and eddy current sensor (*right*)

air purge stream or sealing cutting fluid stream in the measuring gap. Therefore, the eddy current sensor is selected for this project.

## 2.2 Measurement and identification of possible surface deviations

To differentiate between pre-existing geometrical form errors on the part and clamping-conditioned errors, suitable measurement and evaluation procedures need to be developed and adapted. There are various approaches to this topic in literature, which allow to distinguish different causes of form errors from each other and to quantify them. Generally, a distinction has to be drawn between surface deformations that are caused by clamping and are reversible without further machining—i.e. they need to be traced with the tool—and those that are inherent to the workpiece, i.e. they existed before the workpiece was clamped into the chuck.

The procedure is explained with a measurement example. A clamped thin-walled cylinder was measured at a rotation speed of 533 rpm, corresponding to a rotational frequency of approx. 8.9 Hz. Figure 3 shows a test stand, which consists of a light barrier, an eddy current sensor and a hollow cylinder clamped in the chuck jaw. In the measurement range of the light barrier a marking line is drawn on the periphery surface of the jaw chuck. When the light barrier is crossed above the marking line, an impulse signal is sent to and saved in the measuring system. In the following analysis of the measurement data, which describe the deformation of the hollow cylinder, the impulse signals can be used to classify the measurement data into individual areas that correspond to one rotation.

In Fig. 4, each column shows the surface of the workpiece from a different perspective: In the time-coordinate system the entire measurement data were represented as a temporal course, which can be divided into a series of sinus

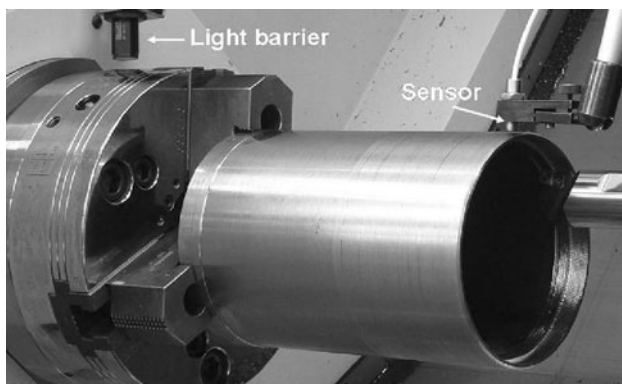


**Fig. 3** Test stand with eddy current sensor

vibrations. In the 3D-coordinate system the measurement data were represented as a surface profile of the workpiece in dependence of the projecting length  $L$  and the shaft angle  $\varphi$ . The polar system provides the comparison between ideal and measured workpiece surface in the single orders.

By means of algorithms developed in MATLAB and MATLAB/SIMULINK, individual orders are filtered from the entire surface deviation and possible deviation types and error causes are identified. For this purpose, very narrow-band elliptical filters are used. The first order represents a clamping error in terms of an eccentric course of the workpiece and a possible tilting of the workpiece in the chuck (axis error), which cause an increasing rotation error (drive) of the workpiece with increasing projection (Fig. 4).

This error needs to be “traced” with the tool. This permits that also workpieces that do not run accurately can be machined, which relaxes the requirements regarding the accuracy of the clamping. Therefore, especially the clamping and readoption of already machined workpieces is considerably facilitated.

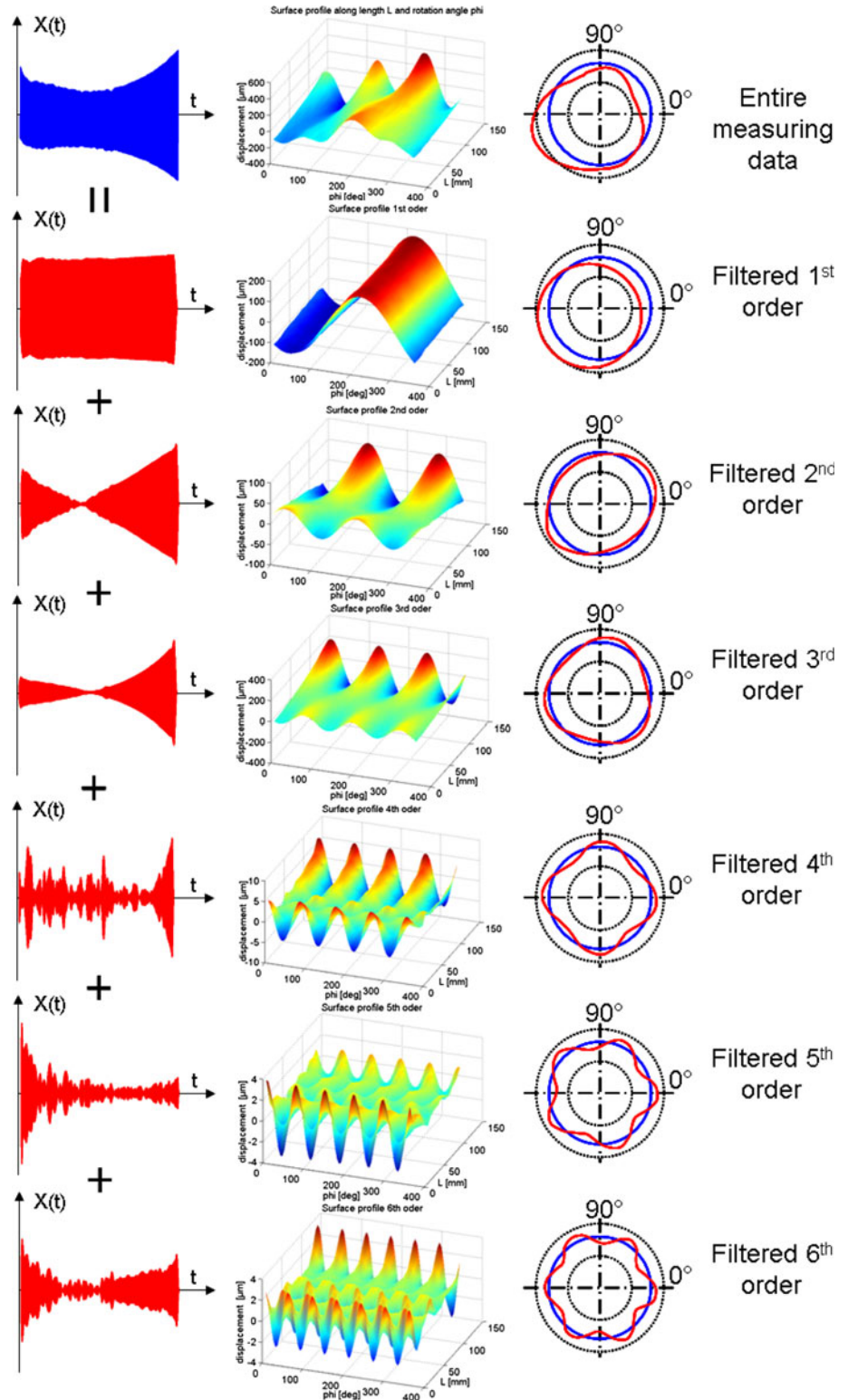
The second order represents a surface error, namely ovality. This error needs to be corrected later. Due to the clamping pressure in the chuck jaw—in the present case three jaws with 120°-distribution and a clamping pressure of 20 bar—the workpiece is deformed trochoidally, which is reflected in the measurement by three waves at the perimeter, i.e. in the third order. It is evident from Fig. 4 that this surface error was only caused by the clamping force. This error needs to be traced with the tool, since this deformation rebounds elastically after unclamping.

Before the tested workpiece was measured, not only the outer surface was machined once, but also the inner surface on a length  $L$  of  $\sim 30$  mm. After the machining, the surface of the workpiece is rough and clearly exhibits chatter marks (Fig. 5). In addition to the waviness of the third order, the workpiece surface, which was measured directly at the cutting point during machining, exhibits a deformation due to the suddenly acting cutting forces. The effects are shown in the fourth, fifth and sixth order, respectively (Fig. 4).

## 2.3 Model-based servo control

The test workpiece was modelled and simulated by means of the finite element method in the FEM program ANSYS. The model enables the calculation of the form deviation due to the clamping in radial  $x$ -direction and hence the calculation of the precontrol values (Fig. 6). It also serves to calculate deformations due to the acting cutting force. The resultant force consists of three individual forces: cutting force  $F_c$ , feed force  $F_f$  and passive force  $F_p$ . First,

**Fig. 4** Measurement and identification of the surface deviation



the calculation model is only established on the basis of the effect of the passive force. An elasticity characteristic diagram can be established from the stiffness matrix of the ideal and clamped workpiece  $N(L, \varphi)$  (Fig. 7) in

dependence of the projection length  $L$  (z-axis in the machine coordinate system) and shaft angle  $\varphi$ . This is done by adding a process force component in the FE-model, on successively all points of the surface, and by calculating



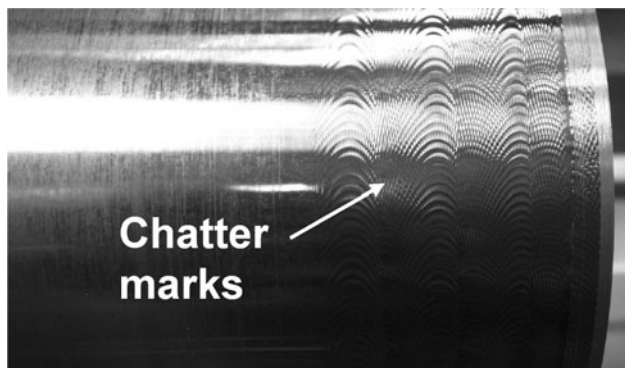


Fig. 5 Workpiece with chatter marks after machining

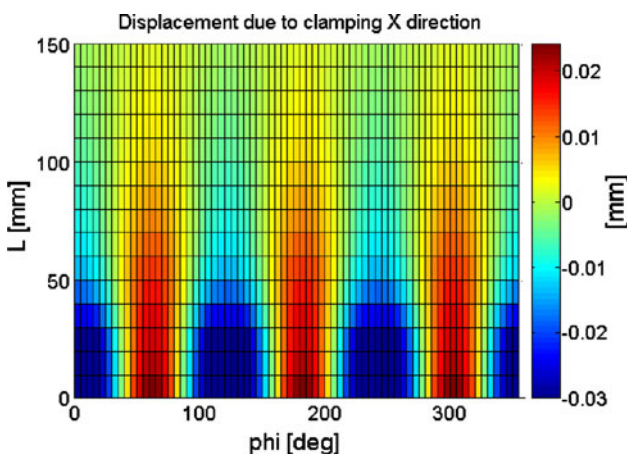


Fig. 6 Displacement due to clamping

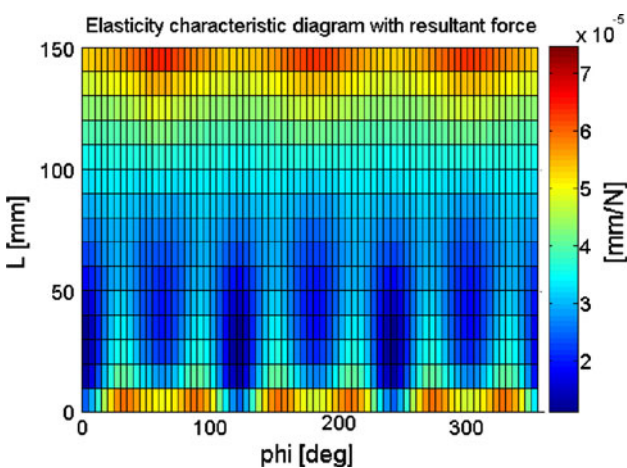


Fig. 7 Elasticity characteristic diagram

the resulting displacement of the point. The elasticity value at this point of the surface is hence

$$N_i(L_i, \varphi_i) = \frac{u_e}{F_e} \tag{1}$$

A simplified action model of the cutting of thin-walled, elastic workpieces can be illustrated schematically in the

form of a closed action circuit according to Fig. 8. The resultant forces are modelled according to the Viktor-Kienzle approach. A quasi-static, stationary behaviour is assumed; the internal dynamics of the involved structures are yet unconsidered [11, 12].

By means of this model the cutting depth  $a_p$  of the clamped ideal workpiece to be machined is calculated and hence the resulting workpiece surface  $x(L, \varphi)$ . Corresponding to the simplified assessment of the acting resultant forces according to Viktor-Kienzle, the workpiece and tool displacements are calculated by means of elasticity characteristic diagrams of the workpiece and the elasticity matrix of the tool. On the basis of these data, correction and precontrol values for the tool path are then determined. In this action model the compensation is also visible. The calculated deformations of the ideal clamped workpiece and the displacements of the workpiece and tool caused by the resultant force were coupled back from the NC program together with the set value in order to close the entire action chain. In the entire cutting process, the deformation of the workpiece plays a substantial and central role in the production of thin-walled parts.

The entering of the correction value causes a workpiece profile difference, compared to the machining without servo control. At the outer projecting end of the workpiece, away from the chuck, indicated with 1, considerably more is fed than without the correction value (Fig. 9, 1 right). At the rear end of the workpiece close to the jaw chuck, indicated with 2, the correction of the trochoidal deformation can be recognised, which is “remachined” with active compensation. In Fig. 10 left, the deformation of the workpiece in clamped state is shown. The largest deformation, here marked in red, is close to the chuck jaw. In Fig. 10 right, an ideal, circular, cylindrical surface of the workpiece is shown after declamping, i.e. after the elastic recovery of the workpiece.

#### 2.4 Integration on the control level

In the implementation of the algorithms on the control level the advantages of the open control platform Siemens 840D of the test machine are used. The algorithms are ported in executable code. The correction value for the x-axis is entered as offset on the interpolator at the outlet of the NC-core. The entire compensation task is implemented in the form of a so-called synchronous action, which synchronises itself onto the interpolator clock pulse of 4 ms. A second possibility arises from the so-called core extension by integrating compile cycles. These are routines, which are completely integrated into the NC-core and passed and processed by the data flow of the channel for the x-axis. The successful implementation of the developed algorithms to the model-based servo control already provides

**Fig. 8** Diagram of a simplified action model

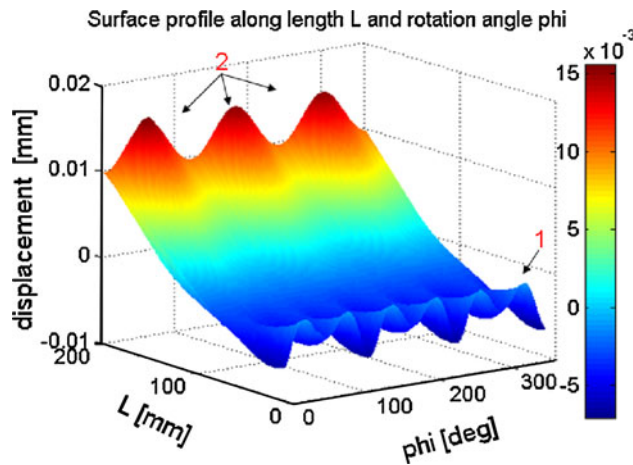
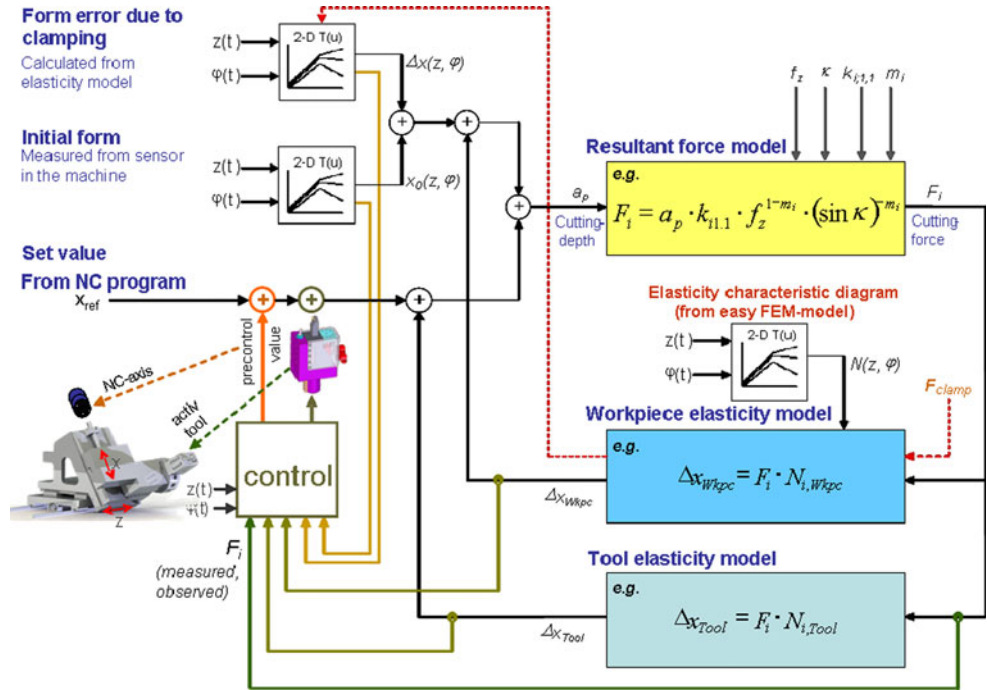


**Fig. 9** Difference profile between machining with and without compensation: unstressed surface with form deviation

an executable system, which can compensate pure form deviations in lower rotational frequencies by means of the machine-inherent direct driven x-axis—completely independent of the additional actuators, such as for example the mechatronic tool holder described below.

### 2.5 Active turning tool holder

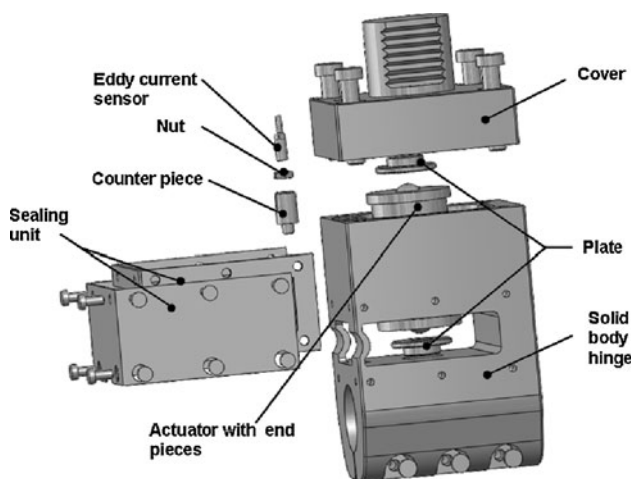
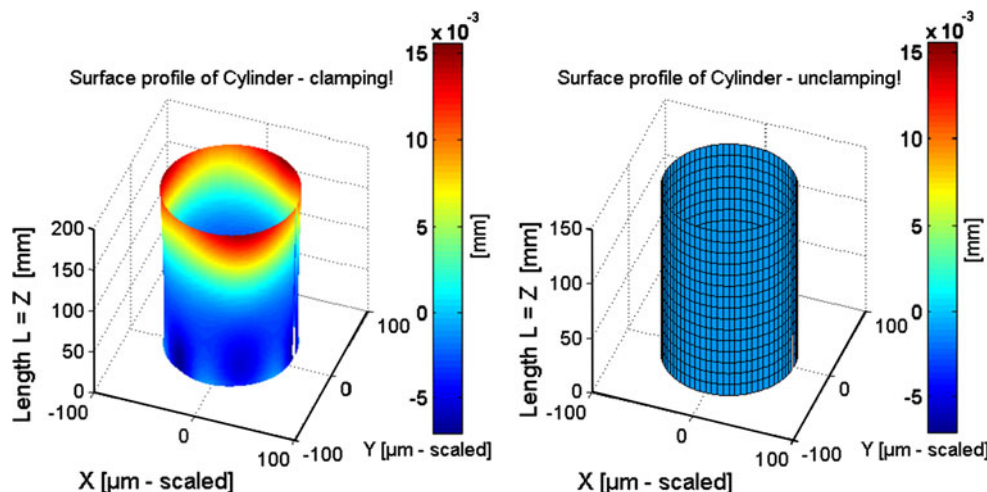
The fast actuator in the tool holder based on a piezo-electric actuator, which is necessary to compensate higher dynamic effects, is designed, optimised and manufactured at the Institute for Machine Tools (IfW).

Figure 11 shows the explosion view of the tool holder. An eddy current sensor is mounted on the solid body hinge and is fixed with a nut. The actuator, on which the end pieces of the ball are fixed, is placed on the lower plate. The cover with the plate placed on solid body hinge, while the actuator is held. The screws in the cover are only tightened slightly at first. By means of the path sensor and the stiffnesses of the actuator and the solid body hinge, the required prestressing force can be accurately determined. After the prestressing was applied to the actuator and the cables were put into the cable routings, the sealing unit was fixed to the solid body hinge in order to isolate chips, cutting fluid, etc.

The active tool holder uses a piezo stack actuator, which exhibits sufficient stroke (60  $\mu\text{m}$ ) for this application. The cutting depth variation is measured with a sensor and fed back into the feed system of the active tool holder by intensifiers after the phase correction. The piezo stroke can be increased by piezo intensifiers (Fig. 12).

To design and dimension the model, simplified elastic multi-body models were derived from the CAD-drafts, by means of which the actuator was statically and dynamically designed for this application with regard to the achievable effective stroke and its frequency response. By means of the finite element models, the design and structure were optimised. Especially when solid body hinges are used, the FEM represents a suitable tool to design the structure both statically and dynamically with regard to fatigue strength.

**Fig. 10** Workpiece surface profile of Cylinder clamping (left), unclamping (right)



**Fig. 11** Explosion view of an active tool holder

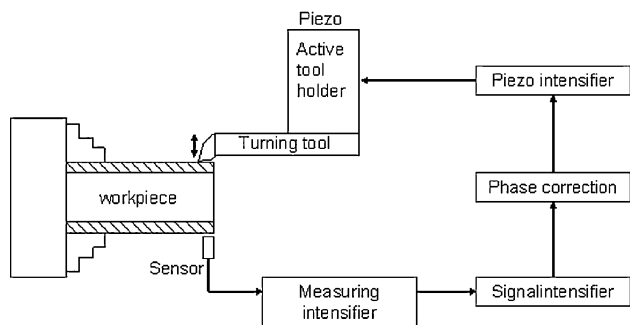


**Fig. 12** Schematic diagram of the action principles of an active tool holder

2.6 Summary

The realisation of the model-based error compensation requires a detailed theoretical investigation. First, models of different modelling depth were designed and experimentally verified by simplified quasi-static assumptions. Besides the

geometrical measurement of the workpieces, errors and elastic clampings, the elasticities of the workpiece and tool were modelled and simulated. Their interaction is described in a cutting model so that also stability investigations of the entire system with regard to form and surface quality of the workpiece can be conducted. The developed models also need to comprise the respective measuring method as well as the actuators including the control in order to enable an optimisation of the production process.

Furthermore, online measurements in the machine will be completed in order to be able to react adaptively to non-ideal workpieces with real inherent errors. In this connection, it is important to have a control circuit to dampen vibrations in the process. The necessary extension of the bandwidth of the mechanical system is achieved by the development of a mechatronic tool or tool holder with integrated actuator.

**Acknowledgments** The financial support by the Baden-Württemberg Stiftung is gratefully acknowledged.

References

1. Zeiher P (2002) Dünnwandige Teile deformationsarm spannen. Flexible Futter mit Spannköpfen fixieren Werkstücke mit hoher Rundlaufgenauigkeit. *MM—Maschinenmarkt* 36:68, 70–71
2. Seegräber L (1992) Standard- oder Sonderausführung? Spannbacken für die Präzisionsbearbeitung in Drehmaschinen. *Schweizer Maschinenmarkt* 92(25):46–48
3. Mayer B (1988) Werkstücke rasch und sicher spannen. Anwendungsbeispiele für Membranspannzeuge 121(2):143–145
4. Imhof H (1995) Vakuum macht's möglich. Spannen dünnwandiger und nichtmagnetischer Werkstücke. *Schweizer Maschinenmarkt* 48:20–21
5. Witte H (1988) Vakuumspanntechnik besonders für neue Werkstoffe und dünnwandige Teile. In: *Technische Keramik*, Vulkan-Verlag, Essen, pp 85–87
6. Walter MF, Stahl JE (1995) Machining of ring shaped work pieces. *J Mater Process Technol* 48(1–4):239–245

7. Spur G, Abelein G, Stelzer C (1993) Force-controlled clamping using three-jaw chucks. *Production Engineering, München* 1(1): 111–116
8. Brinksmeier E, Heinzl C, Nowag L, Sölter J (2003) Simulation der Werkstückdeformation beim Spannen von Ringen. *HTM—Härtereitechnische Mitteilungen* 58(5):271–275
9. Malluck J-A, Melkote S-N (2004) Modeling of deformation of ring shaped workpieces due to chucking and cutting forces. *Transactions of the ASME. J Manuf Sci Eng* 126(10):141–147
10. Qiang L-Z (2000) Finite difference calculation of the deformations of multi-diameter workpieces during turning. *J Mater Process Technol* 98(3):310–316
11. Heisel U, Storchak M (2007) Simulation tool for modelling of interaction process by orthogonal cutting. *Cutting Tool Technol Syst, Kharkov* 73:335–341
12. Heisel U, Krivoruchko DV, Zaloha VA, Storchak M (2007) Cause analysis of errors in FE prediction of orthogonal performances, In: *Proceedings of 10th CIRP international workshop on modeling of machining operations, Calabria, S.* 141–148